

Anion photoelectron spectroscopy of $I_2^-(CO_2)_n$ ($n=1-8$) clusters

Harry Gómez, Travis R. Taylor,^{a)} and Daniel M. Neumark^{b)}

Department of Chemistry, University of California, Berkeley, California 94720, and Chemical Sciences Division, Lawrence Berkeley National Laboratory, Berkeley, California 94720

(Received 12 December 2001; accepted 17 January 2002)

We report the anion photoelectron spectra of $I_2^-(CO_2)_n$ clusters ($n=1-8$) measured at a photon energy of 4.661 eV. Assignment of the spectra is aided by electronic structure calculations on $I_2^-(CO_2)$. The experiment yields size-dependent vertical and adiabatic detachment energies for the formation of the ground state and low-lying valence-excited states of the neutral cluster. Vertical detachment energies are successively blueshifted with increasing cluster size, indicating a stronger stabilization of the anionic cluster relative to the neutral counterpart. In addition, a short progression in the CO_2 bending mode is observed in the $n=1$ and 2 clusters, indicating that the CO_2 solvent species are slightly bent ($\sim 2.5^\circ$) in the anion clusters. The trends in the total and stepwise solvation energies are discussed in terms of cluster geometries solute-solvent interactions. © 2002 American Institute of Physics. [DOI: 10.1063/1.1458246]

I. INTRODUCTION

Molecular clusters offer a unique opportunity to study effects of solvation in chemistry. By investigating clusters in which a chromophore is weakly bound to distinct solvent species, one can follow the evolution of chromophore properties as the number and type of solvent species are varied, with the ultimate goal of understanding how the chromophore spectroscopy and dynamics evolve as one progresses from a gas phase to condensed phase environment. Studies of ionic clusters of this type have proved to be particularly fruitful, because charged clusters can be readily mass-selected, making it relatively straightforward to track cluster properties with size.^{1,2} Anion photoelectron spectroscopy is one of the most versatile techniques for probing size-selected clusters, as it yields energetic and spectroscopic information on both the cluster anion and the neutral cluster formed by photodetachment. In this paper, we report anion photoelectron spectra of $I_2^-(CO_2)_n$ clusters with up to eight CO_2 solvent species.

Clusters of I_2^- are an excellent model system for understanding how the dynamics of a fundamental process, the photodissociation of I_2^- , is affected by clustering. In a series of landmark experiments, Lineberger and co-workers excited the I_2^- chromophore in $I_2^-(CO_2)_n$ and $I_2^-(Ar)_n$ clusters from its $\bar{X}^2\Sigma_u^+$ ground state to the repulsive $\bar{A}'^2\Pi_{g,1/2}$ and $\bar{B}^2\Sigma_g^+$ excited states.³⁻⁹ They observed that a relatively small number of solvent species resulted in caging and recombination of the recoiling $I+I^-$ photofragments, and measured overall time constants for relaxation of the highly vibrationally excited, clustered I_2^- formed by recombination. These experiments are complemented by transient absorption experiments on I_2^- in solution by Barbara and co-workers,^{10,11} and by time-resolved photoelectron spectroscopy

experiments on $I_2^-(CO_2)_n$ and $I_2^-(Ar)_n$ clusters in our group.¹²⁻¹⁷ Molecular dynamics simulations on these clusters have been carried out by Parson,¹⁸⁻²¹ Coker,^{22,23} and co-workers.

However, the interpretation of the dynamics experiments is still somewhat limited by the absence of spectroscopic data on the anion clusters. In particular, experimental information on the solvent binding energies and geometries would be very useful. In addition, in all simulations except one,²⁴ the CO_2 solvent molecules are treated as rigid, linear species, whereas it is known from earlier photoelectron spectroscopy studies^{25,26} that the CO_2 molecules are slightly bent in clusters with atomic halides. It is therefore of interest to determine whether the solute-solvent interaction in $I_2^-(CO_2)_n$ clusters is strong enough to distort the CO_2 geometry.

In the present study, we address these issues by measuring the anion photoelectron spectra of I_2^- and $I_2^-(CO_2)_n$ clusters ($n=1-8$). We describe the experimental setup and the source conditions for the production of $I_2^-(CO_2)_n$ clusters. The spectra show vibrational structure indicating that the CO_2 molecules are slightly bent in the anion clusters. The observed shifts of the bands in the photoelectron spectra with increasing solvation are discussed in terms of possible cluster geometries and changes in solvation energy as a function of cluster size and electronic state. Electronic structure calculations have been carried out on I_2^- , $I_2^-(CO_2)$, and $I_2^-(CO_2)_2$ to aid in the interpretation of the anion photoelectron spectra.

II. EXPERIMENT

The negative ion time-of-flight (TOF) photoelectron (PE) spectrometer used in this study has been described in detail previously.^{27,28} Briefly, $I_2^-(CO_2)_n$ clusters are prepared by coexpanding iodine vapor with 4-40 psi of a 5% CO_2/Ar mixture at room temperature through a pulsed molecular beam valve with a ~ 0.75 -mm-diam orifice. The valve is operated at a repetition rate of 20 Hz. Negative ions are gener-

^{a)}Current address: Lam Research, 47131 Bayside Parkway, Fremont, CA 94538.

^{b)}Electronic mail: dan@radon.cchem.berkeley.edu

ated by a 1 keV, 300 mA electron beam that crosses the gas jet just downstream of the nozzle, in the continuum flow region of the expansion. The ions are extracted perpendicularly to the expansion by means of a pulsed electric field into a linear reflection TOF mass spectrometer at an average beam energy of 2.5 keV. The mass resolution is $m/\Delta m = 2000$. At the spatial focus of the mass spectrometer, ions are intersected and photodetached by a fixed frequency laser pulse from a Nd:YAG laser running at 20 Hz. The laser firing delay with respect to the pulsed extraction field is varied until optimal temporal overlap is achieved with the ions of the desired mass. The fourth harmonic of the Nd:YAG laser at 266 nm (4.661 eV) was used in the present study.

Photodetached electrons are detected at the end of a 1 m magnetically shielded flight tube, mounted orthogonally to the laser and ion beam, and are energy analyzed by TOF. The electron detector, a 75-mm-diam chevron microchannel plate configuration with a flat anode, subtends a solid angle of 0.0044 sr, so that 0.035% of the detached photoelectrons are detected. The instrumental resolution is 8–10 meV for an electron kinetic energy (eKE) of 0.65 eV and degrades as $(\text{eKE})^{3/2}$. Under typical conditions, the ion density in the laser interaction region is about $10^5/\text{cm}^3$ for I_2^- and decreases with increasing cluster size. Approximately 30% of the ions are photodetached at 266 nm and about one electron is detected per laser shot. A typical spectrum requires 300, 000–600, 000 laser shots. Ultraviolet photons efficiently eject electrons from metal surfaces, resulting in a residual background photoelectron contribution of typically one electron per ten laser shots at 266 nm, primarily at low eKE. Background spectra were recorded on a daily basis, summed, and then subtracted from the acquired data.

All photoelectron spectra presented here are plotted as a function of the electron kinetic energy (eKE, bottom axis) and electron binding energy (eBE, top axis), where

$$\text{eBE} = h\nu - \text{eKE} \quad (1)$$

and $h\nu$ is the photon energy of the detachment laser. The angle between the laser polarization and the direction of electron collection can be varied by means of a half-wave plate. All spectra reported here were measured at a laser polarization angle of 90° .

III. RESULTS

A. Photoelectron spectra

The anion PE spectra of I_2^- and $\text{I}_2^-(\text{CO}_2)$ at 266 nm are shown in Fig. 1. The bare I_2^- spectrum is comprised of transitions to six electronic states of I_2 with energies centered at eKE = 1.422 eV (X), 0.875 eV (A'), 0.783 eV (A), 0.533 eV (B'), 0.422 eV (B''), and 0.239 eV (B), where the band labeling corresponds to the accepted notation for the I_2 electronic states. The corresponding vertical detachment energies (VDEs), defined as the electron binding energy at each band maximum, are 3.235 eV (X), 3.782 eV (A'), 3.874 eV (A), 4.124 eV (B'), 4.235 eV (B''), and 4.235 eV (B). Vibrational structure is observed in the X, A' , and A bands, but

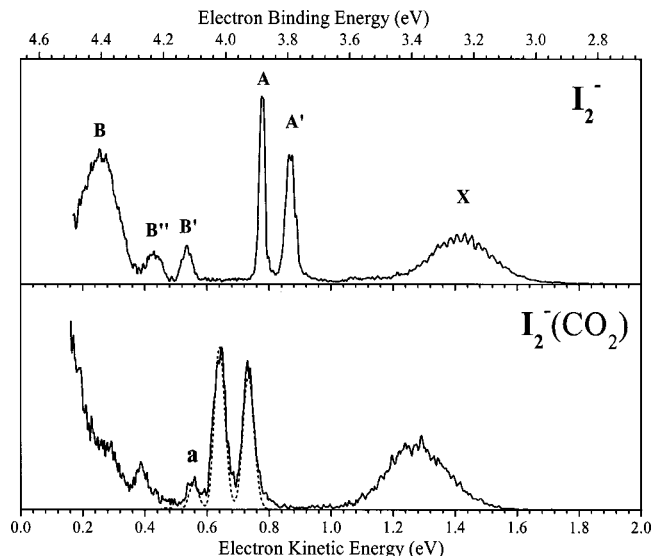


FIG. 1. Anion photoelectron spectra (solid) of I_2^- and $\text{I}_2^-(\text{CO}_2)$ measured at photon energy of 4.661 eV (266 nm). Franck–Condon simulation (dashed) of bands A' and A of the $\text{I}_2^-(\text{CO}_2)$ spectrum is also shown.

this structure is less resolved than in the previously reported PE spectrum of I_2^- at 355 nm²⁹ due to lower electron energy resolution at higher eKE.

The $\text{I}_2^-(\text{CO}_2)$ PE spectrum has the same general appearance as the bare I_2^- spectrum. Five of the six electronic bands (i.e. all except B) appear in the $\text{I}_2^-(\text{CO}_2)$ spectrum, but the VDEs for these bands are all higher by 135–140 meV. Band X in the I_2^- spectrum is wider than the corresponding band in the $\text{I}_2^-(\text{CO}_2)$ spectrum. This effect is attributed to fewer vibrational hot bands in the cluster PE spectrum, and has been seen in previous PE spectra of $\text{I}_2^-(\text{Ar})$ and $\text{I}_3^-(\text{Ar})$.^{30,31} In contrast, bands A' and A in $\text{I}_2^-(\text{CO}_2)$ are considerably broader than their counterparts in the bare I_2^- spectrum, and a new feature, band a, appears at 80 meV ($\sim 670 \text{ cm}^{-1}$) lower eKE than band A; this spacing is close to the bending frequency of CO_2 (667 cm^{-1}).

The 266 nm PE spectra of $\text{I}_2^-(\text{CO}_2)_n$ ($n = 0-8$) clusters are shown in Fig. 2. The spectra of these clusters remain similar in form, except for a continuous shift of all bands to lower eKE, i.e., higher electron binding energy (eBE). While band X remains mostly unchanged with the addition of the CO_2 molecules, bands A and A' become noticeably broader. Peak a in the $\text{I}_2^-(\text{CO}_2)$ spectrum appears as a small shoulder in the $\text{I}_2^-(\text{CO}_2)_2$ spectra and it disappears and/or is overlapped in the larger clusters by the broadening of bands A' and A. The $n = 6$ cluster is the largest for which both bands A' and A are energetically accessible at 266 nm, whereas the weaker bands B' and B'' are out of range for $n > 2$.

The shifts in VDE for bands X, A, A' , and B' are listed in Table I. These shifts are determined by horizontally displacing the band of interest to achieve the best overlap with the corresponding feature in the $\text{I}_2^-(\text{CO}_2)$ spectrum. Table I shows the total shifts relative to I_2^- as well as the stepwise shifts (in parentheses) relative to $\text{I}_2^-(\text{CO}_2)_{n-1}$, i.e., the shift from the addition of the n th CO_2 molecule. The estimated error bars for the energy shifts are ± 7 meV for bands A' , A, and B' and ± 10 meV for band X.

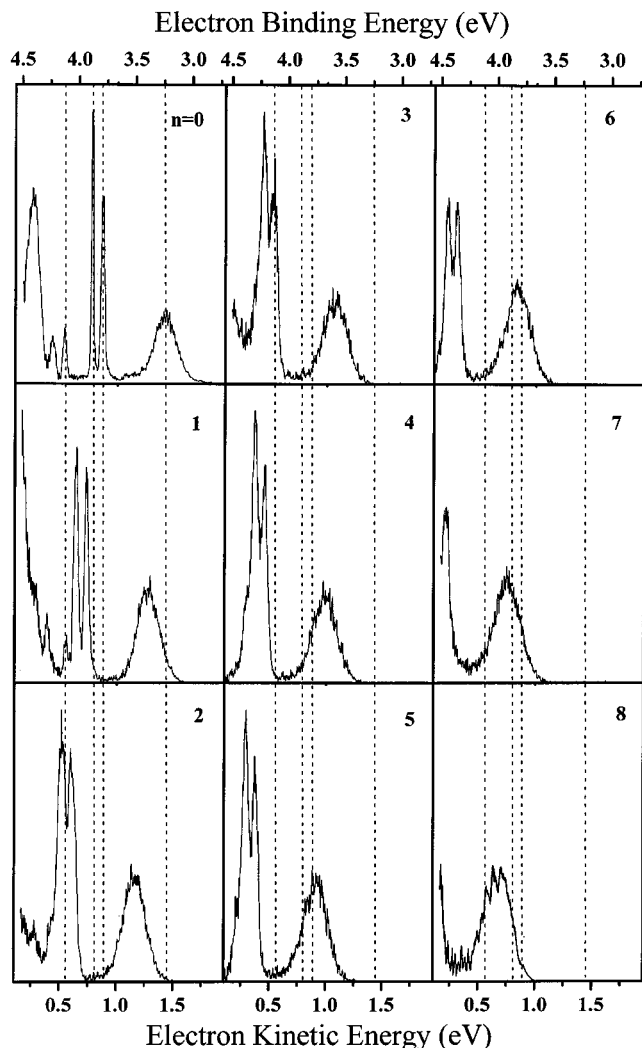


FIG. 2. Anion photoelectron spectra of $I_2^-(CO_2)_n$ clusters measured at a photon energy of 4.661 eV. The vertical detachment energies for the formation of the X , A' , A , and B' states of bare I_2 are indicated by the broken vertical lines.

B. Electronic structure calculations

Electronic structure calculations were performed to assist in the interpretation of the data presented previously. These calculations are aimed at determining the geometries of the binary $I_2^-(CO_2)$ and $I_2 \cdot (CO_2)$ complexes. I_2/I_2^- and

TABLE I. Total and stepwise shifts (in parentheses) of the bands in the photoelectron spectra of $I_2^-(CO_2)_n$ clusters relative to the I_2^- spectrum as a function of cluster size n . All energies are in meV.

| n | $X(^1\Sigma_g^+)$ | $A'(^3\Pi_{2u})$ | $A(^3\Pi_{1u})$ | $B'(^3\Pi_{0-u})$ |
|-----|-------------------|------------------|-----------------|-------------------|
| 0 | 0 | 0 | 0 | 0 |
| 1 | 139 (+139) | 136 (+136) | 135 (+135) | 140 (+140) |
| 2 | 250 (+111) | 260 (+124) | 260 (+125) | 255 (+115) |
| 3 | 345 (+95) | 339 (+79) | 340 (+80) | |
| 4 | 425 (+80) | 420 (+81) | 415 (+75) | |
| 5 | 500 (+75) | 492 (+72) | 483 (+68) | |
| 6 | 580 (+80) | 569 (+77) | 559 (+76) | |
| 7 | 662 (+82) | 661 (+92) | | |
| 8 | 745 (+83) | | | |

$I_2/I_2^-(CO_2)$ geometries were optimized at the unrestricted Hartree–Fock (UHF) and HF levels of theory for the anion and neutral, respectively, then further explored using second-order Møller–Plesset (MP2), and density functional theory with the Becke–three-parameter–Lee–Yang–Parr (B3LYP) exchange correlation functional.^{32,33} The STO-3G*, and 6-311** basis sets were used. Calculations were performed using GAUSSIAN98 electronic structure package,³⁴ and the results are summarized in Table II. Experimental data on CO_2 , I_2 , and I_2^- are included in Table II for comparison.^{29,35,36}

Several configurations for the anion complex were explored at UHF/STO-3G* and UHF/6-311G**, but only the global minimum structure is reported and studied further at higher levels of theory. This structure, shown in Fig. 3, has C_{2v} symmetry, with the CO_2 molecule lying in the plane that bisects the I–I bond. This structure is similar to previous structures calculated using Monte Carlo¹⁸ and molecular dynamics³⁷ simulations. However, the electronic structure calculations at all levels of theory predict that the CO_2 in $I_2^-(CO_2)$ is slightly bent, with a deviation from linearity of $\sim 2.6^\circ$ to $\sim 5.7^\circ$ depending on the level of theory. In Table II, the “experimental” result for the bond angle is based on the Franck–Condon analysis described in Sec. IV.

The neutral $I_2(CO_2)$ cluster has a local minimum structure similar to the global minimum for the anion. The major differences are that the CO_2 is very nearly linear in the neutral complex, and the distance between the C atom and the I_2 center-of-mass, R_{I-C} in Table II, is considerably longer. Both effects are consistent with a weaker intermolecular interaction in the neutral complex.

Table II shows that the agreement between the experimental and calculated I_2^- geometries and frequencies is considerably better in the MP2 than in the B3LYP calculation, while for neutral I_2 both calculations compare equally well with experiment. The MP2/6-311G** and B3LYP/6-311G** calculations show that the bond lengths of bare I_2^- and I_2 are essentially unchanged upon complexation with CO_2 , and R_{C-O} in the neutral and anion clusters is very close to the experimental value for bare CO_2 . The CO_2 is slightly more bent in the B3LYP/6-311G** calculation (176.1° versus 176.6°). The biggest difference between the two calculations is that R_{I-C} is noticeably larger for the anion and neutral complexes in the B3LYP/6-311G** calculation, as is the increase in R_{I-C} upon photodetachment (1.256 versus 0.357 \AA). Vibrational frequencies for the anion and neutral complexes were calculated at the MP2/6-311G** and B3LYP/6-311G** level of theory and the results for the three totally symmetric modes from the MP2/6-311G** calculation are included in Table II. MP2/6-311G** population analysis of the $I_2^-(CO_2)$ complex indicates that $\sim 1.7\%$ of the total negative charge has migrated from the I_2^- anion to the CO_2 molecule. The CO_2 distortion is correlated with the degree of charge transfer, which ranges from 0.3% to 2.0% depending upon the level of theory. However, distortion of the CO_2 can also result purely from electrostatic effects, as discussed in previous work on $X^-(CO_2)$ clusters.²⁶

TABLE II. Results of electronic structure calculations for $I_2^-(CO_2)$ and $I_2(CO_2)$. All bond lengths in Å. Vibrational frequencies in cm^{-1} for the totally symmetric modes of $I_2^-(CO_2)/I_2(CO_2)$ are (59/41, 110/224, 598/612, 1332/1330) from MP2/6-311G** calculation.

| Species | Level of theory | R_{I-I} | R_{C-O} | R_{I-C} | $\angle OCO$ ($^\circ$) |
|-----------------|-----------------|--------------------|--------------------------|-----------|---------------------------|
| $I_2^-(CO_2)$ | UHF/STO-3G* | 3.088 24 | 1.188 43 | 3.2464 | 174.284 |
| | MP2/STO-3G* | 3.072 15 | 1.230 00 | 3.4111 | 177.441 |
| | UHF/6-311G** | 3.350 77 | 1.135 66 | 3.8436 | 176.833 |
| | MP2/6-311G** | 3.284 06 | 1.169 00 | 3.4413 | 176.560 |
| | B3LYP/6-311G** | 3.392 61 | 1.161 40 | 3.9702 | 176.104 |
| CO ₂ | Experiment | | 1.162 1 ^a | | 177.5 ^b |
| $I_2(CO_2)$ | HF/STO-3G* | 2.581 53 | 1.187 94 | 4.3963 | 179.941 |
| | MP2/STO-3G* | 2.579 85 | 1.230 84 | 3.9436 | 179.959 |
| | HF/6-311G** | 2.703 17 | 1.135 27 | 4.7373 | 179.876 |
| | MP2/6-311G** | 2.714 95 | 1.169 04 | 3.7983 | 179.810 |
| | B3LYP/6-311G** | 2.736 83 | 1.160 84 | 5.2261 | 179.874 |
| CO ₂ | Experiment | | 1.162 1 ^a | | 180.0 |
| | | R_{I-I} | ω_e (cm^{-1}) | | |
| I_2^- | MP2/6-311G** | 3.284 90 | 109.22 | | |
| | B3LYP/6-311G** | 3.402 81 | 83.53 | | |
| | Experiment | 3.205 ^c | 110 ^c | | |
| I_2 | MP2/6-311G** | 2.714 41 | 222.15 | | |
| | B3LYP/6-311G** | 2.736 93 | 206.55 | | |
| | Experiment | 2.666 ^d | 214.57 ^d | | |

^aReference 35.^bThis work.^cReference 29.^dReference 36.

IV. ANALYSIS AND DISCUSSION

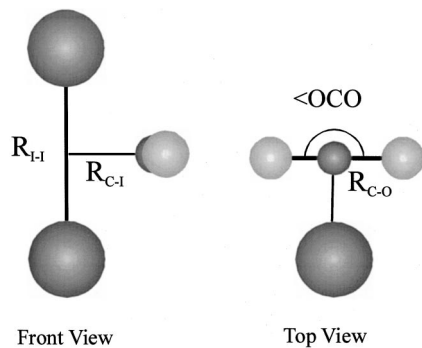
In this section, we first focus on the geometries of the $I_2^-(CO_2)$ and $I_2(CO_2)$ binary complexes by a Franck–Condon analysis of the photoelectron spectrum in Fig. 1. We then analyze and discuss the cluster energetics as revealed by the PE spectra in Fig. 2.

A. Franck–Condon analysis

We have performed Franck–Condon simulations of bands *A* and *A'* in the $I_2^-(CO_2)$ and $I_2^-(CO_2)_2$ PE spectra in order to analyze the new feature (*a*) in the spectra and to characterize the vibrational temperature of the negative ions. The simulations are superimposed on the $I_2^-(CO_2)$ PE spectrum in Fig. 1, and are largely based on the MP2/6-311G** results in Table II, since this calculation yielded significantly

better I_2^- parameters than the B3LYP/6-311G** calculation. Using the calculated MP2/6-311G** geometries, frequencies and force constants for the anion and neutral ground state complex, and experimental frequencies and distances for the I_2 *A* and *A'* electronic states,^{38,39} we have simulated the photoelectron spectra within the parallel mode approximation using three totally symmetric vibrational modes: the I–I stretch, the CO₂ bend and the low-frequency I–C stretch motion. The CO₂ bending angle and frequency and the anion temperature were optimized in order to reproduce the spectra. The change in normal coordinate for the low frequency I–C stretch was set at the value obtained from the MP2/6-311G** geometries; we assumed this displacement is independent of the neutral I_2 electronic state.

The parameters determined from the fit are 680 ± 20 cm^{-1} for the CO₂ bend frequency, $177.5 \pm 1.0^\circ$ for the OCO bend angle, and 80 ± 20 K for the cluster temperature. The CO₂ frequency and bend angle were chosen to reproduce the position and intensity of band *a*. The simulations confirm that peak *a* is due to excitation of one quantum of the CO₂ bend in the neutral complex with I_2 in its *A* state. In principle, similar features should be associated with each neutral state of I_2 accessed in the photoelectron spectra. However, the analogous feature associated with band *A'* lies under band *A*, and for band *X* it is obscured by the extended progression in the I–I stretch. The simulations also show that the broadening of bands *A* and *A'* relative to the bare I_2^- spectrum is mainly due to vibrational activity in the I–C stretch due to the increase in R_{I-C} upon photodetachment; this broadening is reproduced satisfactorily using ΔR_{I-C}

FIG. 3. Lowest energy calculated structure for $I_2^-(CO_2)$ based on results from Table II.

$=0.357 \text{ \AA}$ from the MP2/6-311G** calculation.

The OCO bend angle obtained from our Franck-Condon analysis is slightly larger than that obtained from the two highest level calculations in Table II, possibly reflecting the need for more diffuse functions in the basis sets used in the anion calculations. The CO_2 in $I_2^-(CO_2)$ is more linear than in the $I^- \cdot CO_2$ complex, for which the CO_2 angle is $174.5 \pm 1.5^\circ$.²⁶ This result may reflect the delocalization if the I_2^- charge is over the two centers, reducing the effective potential between the charge and the CO_2 quadrupole. Although the analog of peak *a* is not clearly resolved in PE spectra of the larger clusters, these spectra do show a shoulder where this peak would be expected, so we expect bent CO_2 molecules to be present in the larger clusters as well.

B. Cluster energetics

As has been discussed in earlier work,^{25,30} the shifts in the VDEs with number of CO_2 molecules in Table I are a measure of the differences in anion and neutral solvent binding energies. The positive shifts with increasing n seen here indicate that binding in the anion is stronger than in the neutral, as expected, since the leading $-1/r^3$ charge-quadrupole attractive term in the anion is absent in the neutral.

More quantitatively, the shifts can be interpreted in terms of the stepwise solvation energies $SE_{\text{step}}^i(n)$ and $SE_{\text{step}}^-(n)$, defined as the solvent dissociation energies for the loss of a single CO_2 molecule from $I_2 \cdot (CO_2)_n$ or $I_2^- \cdot (CO_2)_n$, respectively; the superscript *i* indicates the I_2 neutral electronic state. The total solvation energy $SE_{\text{tot}}(n)$, defined for the anion and neutral clusters, is given by the sum over the stepwise solvation energies $SE_{\text{step}}(x)$:

$$SE_{\text{tot}}(n) = \sum_{x=1}^n SE_{\text{step}}(x). \quad (2)$$

The VDEs are related to the stepwise solvation energy difference $\Delta SE_{\text{step}}^i(n)$, i.e., the difference in the stepwise solvation energy of the neutral, $SE_{\text{step}}^i(n)$, and of the anionic cluster, $SE_{\text{step}}^-(n)$, as follows:

$$\begin{aligned} VDE^i(n) - VDE^i(n-1) &= SE_{\text{step}}^-(n) - SE_{\text{step}}^i(n) \\ &\equiv \Delta SE_{\text{step}}^i(n). \end{aligned} \quad (3)$$

The total solvation energy difference $\Delta SE_{\text{tot}}^i(n)$ is then given by

$$VDE^i(n) - VDE^i(0) = \sum_{x=1}^n \Delta SE_{\text{step}}^i(x) \equiv \Delta SE_{\text{tot}}^i(n). \quad (4)$$

Strictly speaking, one should use adiabatic detachment energies (ADEs) rather than VDEs in Eqs. (3) and (4), where the ADE is defined as the energy gap between the vibrational ground states of the anion and neutral electronic state in question (and is equal to the electron affinity when the neutral electronic state is the ground state). Accurate determination of ADEs is difficult in the absence of resolved vibrational structure in the PE spectrum. Since the addition of CO_2 solvent molecules results in relatively minor changes in

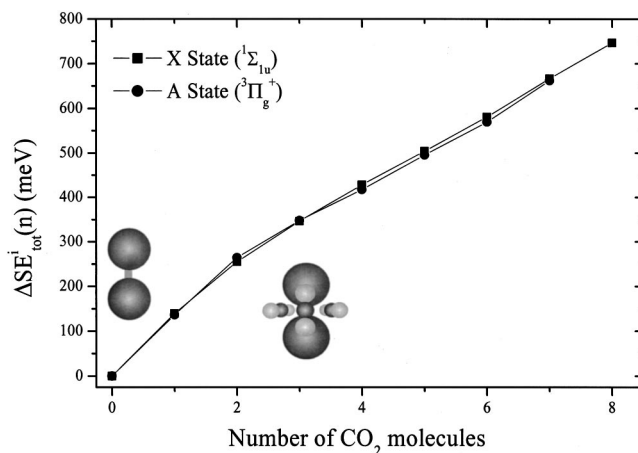


FIG. 4. Total solvation energy difference $\Delta SE_{\text{tot}}^i(n)$ for detachment to the X and A states of $I_2(CO_2)_n$ as a function of cluster size n .

the shape of each band, we assume that the shifts in ADEs are equal to the shifts in the VDEs and use the latter in Eqs. (3) and (4).

In Fig. 4, the total solvation energy differences for the A and X states, $\Delta SE_{\text{tot}}^A(n)$ and $\Delta SE_{\text{tot}}^X(n)$, are plotted as a function of cluster size. $\Delta SE_{\text{tot}}^A(n)$ is essentially identical to $\Delta SE_{\text{tot}}^X(n)$ and has therefore been omitted from Fig. 4. The small differences between $\Delta SE_{\text{tot}}^A(n)$ and $\Delta SE_{\text{tot}}^X(n)$ may not be significant. For all three states, $\Delta SE_{\text{tot}}^i(n)$ increases monotonically with cluster size, but the slope drops considerably above $n=2$. At $n=8$, the largest cluster studied, the anion cluster is stabilized by 745 meV relative to the neutral cluster in the X state.

Trends in the solvation energies are emphasized by plotting the stepwise solvation energy difference for the X state, $\Delta SE_{\text{step}}^X(n)$, as a function of the cluster size n in Fig. 5. The first CO_2 molecule is bound by 139 meV more strongly in the anion than in the neutral. $\Delta SE_{\text{step}}^X(n)$ decreases steadily from $n=1$ to $n=4$ and then remains nearly constant from $n=4$ to 8, over which range each CO_2 stabilizes the anion by ~ 80 meV relative to the neutral.

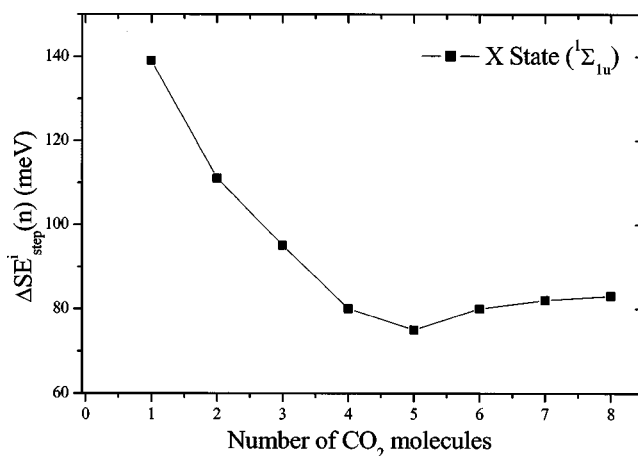


FIG. 5. Stepwise solvation energy difference $\Delta SE_{\text{step}}^X(n)$ for detachment to the X state of $I_2(CO_2)_n$ as a function of cluster size n .

The results in Fig. 5 differ significantly from those seen previously for $I_2^- Ar_n$ and $IHI^- Ar_n$ clusters,^{30,40} for which $\Delta SE_{\text{step}}(n)$ was relatively constant for the first six Ar atoms and then decreased sharply. The earlier results were consistent with molecular dynamics simulations on $I_2^- Ar_n$ clusters^{21,41} that predicted the first six Ar atoms form a ring around the waist of the anion core, allowing each Ar atom to interact strongly with the partial negative charge residing on each Ar atom. Subsequent Ar atoms can be adjacent to only a single I atom, hence their binding energy in the anion is lowered.

The $\Delta SE_{\text{step}}(n)$ trends in $I_2^- Ar_n$ clusters were interpreted largely in terms of effects in the anion rather than the neutral clusters, and it is reasonable to make the same assumption for $I_2^-(CO_2)_n$ clusters. In other words, we attribute the steep drop in $\Delta SE_{\text{step}}^X(n)$ in Fig. 5 for $n=1-4$ to decreases in $SE_{\text{step}}^-(n)$ over this size range, so that the first CO_2 binds the most strongly in the anion, with each successive CO_2 binding less strongly until $n=4$, above which the binding energies are relatively constant. This interpretation is justified in part because the anion binding energies are stronger than the neutral binding energies, so that one would expect larger absolute variations with n in $SE_{\text{step}}^-(n)$ than in $SE_{\text{step}}^X(n)$.

One can then view the overall trend in Fig. 5 as a competition between $I_2^- \cdot CO_2$ interactions and $CO_2 \cdot CO_2$ interactions. The $I_2^- \cdot CO_2$ interaction is most favorable for the geometry in Fig. 3, which maximizes the attraction between the partial positive charge on the carbon atom and the negatively charged I atoms while minimizing the repulsion between the partial negative charges on the O and I atoms. On the other hand, in CO_2 dimer, the two CO_2 's are parallel but displaced in order to maximize attraction between the electropositive C atom and electronegative O atoms.⁴²⁻⁴⁴ Hence, if the first two or three CO_2 molecules added to the I_2^- are aligned to lie in the plane that bisects the I_2^- bond, as predicted in the simulations by Amar and Perera,³⁷ they will be in an unfavorable orientation with respect to one another because of the proximity of the O atoms in adjacent CO_2 molecules, resulting in a progressively lower binding energy as more CO_2 molecules are added. Note that in $I^-(CO_2)_n$ clusters,²⁵ where there is no I_2^- axis to align the CO_2 molecules, the solvent shifts are relatively flat for the first several CO_2 molecules, lying between 140 and 150 meV for $n=1-4$. The flattening in Fig. 5 for $n>4$ suggests that subsequent CO_2 molecules primarily interact with one rather than two I atoms, so that the alignment with respect to the I_2^- axis is less important than in the smaller clusters. This interpretation is consistent with molecular dynamics simulations of the structures of the larger cluster anions.^{18,22,37} Given the large variation of binding energies, one might certainly expect different distortions from linearity for the inequivalently bound solvent molecules.

According to Eqs. (3) and (4), the photoelectron spectra are sensitive only to the differences in the anion and neutral solvent binding energies. Hence, more experimental information is needed to extract the actual anion/neutral solvation energies. Papanikolas *et al.*⁴ found that excitation of $I_2^-(CO_2)_n$ clusters at 720 nm (1.75 eV) results in the loss of seven CO_2 molecules from clusters with $10 < n < 22$, yielding

an average binding energy of 0.25 eV. However, aside from being an average value, it is also an upper bound, because each CO_2 molecules leaves with nonzero kinetic energy. More recently, we have used femtosecond stimulated emission pumping (FSEP) to vibrationally excite the I_2^- chromophore in $I_2^-(CO_2)_n$ clusters and observe the number of CO_2 molecules that evaporate over a wide range of vibrational excitation energies.⁴⁵ The FSEP results, when combined with the VDE shifts measured here, yield a best-fit solvent binding energy of $SE_{\text{step}}=95$ meV for neutral $I_2^-(CO_2)_n$ clusters, assumed to be independent of n , so that in the anion clusters, $SE_{\text{step}}^-(n)=234$ meV for the first CO_2 and 178 meV for the eighth CO_2 . Details of this analysis are presented in the FSEP paper.

V. CONCLUSIONS

The photoelectron spectra of $I_2^-(CO_2)_n$ clusters presented here yield new insights into the structure and energetics of these clusters. The spectra show that the interaction between the I_2^- and CO_2 constituents of the cluster is sufficient to distort the CO_2 from linearity, and this distortion is reproduced in electronic structure calculations on the binary $I_2^-(CO_2)$ complex. Franck-Condon simulations of the $I_2^-(CO_2)$ spectrum show this distortion is only 2.5° , but inclusion of this distortion may be desirable in future molecular dynamics simulations of structures and energetics of larger $I_2^-(CO_2)_n$ clusters. The PE spectra also yield trends in cluster energetics through shifts in the vertical detachment energies with increasing cluster size, implying that in the anion clusters, the binding energy of each successive CO_2 drops significantly for the first four solvent molecules, after which little variation occurs. This drop in binding energy is attributed to competing I_2^-/CO_2 and CO_2/CO_2 interactions.

ACKNOWLEDGMENT

This research is supported by the Air Force Office of Scientific Research under Grant No. F49620-00-1-0145.

- ¹A. W. Castleman, Jr. and K. H. Bowen, Jr., *J. Phys. Chem.* **100**, 12911 (1996).
- ²M. A. Duncan, *Int. J. Mass. Spectrom.* **200**, 545 (2000).
- ³D. Ray, N. E. Levinger, J. M. Papanikolas, and W. C. Lineberger, *J. Chem. Phys.* **91**, 6533 (1989).
- ⁴J. M. Papanikolas, J. R. Gord, N. E. Levinger, D. Ray, V. Vorsa, and W. C. Lineberger, *J. Phys. Chem.* **95**, 8028 (1991).
- ⁵J. M. Papanikolas, V. Vorsa, M. E. Nadal, P. J. Campagnola, H. K. Buchenau, and W. C. Lineberger, *J. Chem. Phys.* **99**, 8733 (1993).
- ⁶J. M. Papanikolas, V. Vorsa, M. E. Nadal, P. J. Campagnola, J. R. Gord, and W. C. Lineberger, *J. Chem. Phys.* **97**, 7002 (1992).
- ⁷V. Vorsa, P. J. Campagnola, S. Nandi, M. Larsson, and W. C. Lineberger, *J. Chem. Phys.* **105**, 2298 (1996).
- ⁸V. Vorsa, S. Nandi, P. J. Campagnola, M. Larsson, and W. C. Lineberger, *J. Chem. Phys.* **106**, 1402 (1997).
- ⁹A. Sanov, T. Sanford, S. Nandi, and W. C. Lineberger, *J. Chem. Phys.* **111**, 664 (1999).
- ¹⁰A. E. Johnson, N. E. Levinger, and P. F. Barbara, *J. Phys. Chem.* **96**, 7841 (1992).
- ¹¹P. K. Walhout, J. C. Alfano, K. A. M. Thakur, and P. F. Barbara, *J. Phys. Chem.* **99**, 7568 (1995).
- ¹²B. J. Greenblatt, M. T. Zanni, and D. M. Neumark, *Science* **276**, 1675 (1997).
- ¹³B. J. Greenblatt, M. T. Zanni, and D. M. Neumark, *Faraday Discuss.* **108**, 101 (1997).

- ¹⁴B. J. Greenblatt, M. T. Zanni, and D. M. Neumark, *J. Chem. Phys.* **112**, 601 (2000).
- ¹⁵B. J. Greenblatt, M. T. Zanni, and D. M. Neumark, *J. Chem. Phys.* **111**, 10566 (1999).
- ¹⁶A. V. Davis, M. T. Zanni, C. Frischkorn, M. Elhanine, and D. M. Neumark, *J. Electron Spectrosc. Relat. Phenom.* **112**, 221 (2000).
- ¹⁷D. M. Neumark, *Annu. Rev. Phys. Chem.* **52**, 255 (2001).
- ¹⁸J. M. Papanikolas, P. E. Maslen, and R. Parson, *J. Chem. Phys.* **102**, 2452 (1995).
- ¹⁹N. Delaney, J. Faeder, P. E. Maslen, and R. Parson, *J. Phys. Chem. A* **101**, 8147 (1997).
- ²⁰J. Faeder, N. Delaney, P. E. Maslen, and R. Parson, *Chem. Phys.* **239**, 525 (1998).
- ²¹J. Faeder and R. Parson, *J. Chem. Phys.* **108**, 3909 (1998).
- ²²V. S. Batista and D. F. Coker, *J. Chem. Phys.* **106**, 7102 (1997).
- ²³C. J. Margulis and D. F. Coker, *J. Chem. Phys.* **110**, 5677 (1999).
- ²⁴B. M. Ladanyi and R. Parson, *J. Chem. Phys.* **107**, 9326 (1997).
- ²⁵D. W. Arnold, S. E. Bradforth, E. H. Kim, and D. M. Neumark, *J. Chem. Phys.* **102**, 3510 (1995).
- ²⁶D. W. Arnold, S. E. Bradforth, E. H. Kim, and D. M. Neumark, *J. Chem. Phys.* **102**, 3493 (1995).
- ²⁷R. B. Metz, A. Weaver, S. E. Bradforth, T. N. Kitsopoulos, and D. M. Neumark, *J. Phys. Chem.* **94**, 1377 (1990).
- ²⁸C. Xu, G. R. Burton, T. R. Taylor, and D. M. Neumark, *J. Chem. Phys.* **107**, 3428 (1997).
- ²⁹M. T. Zanni, T. R. Taylor, B. J. Greenblatt, B. Soep, and D. M. Neumark, *J. Chem. Phys.* **107**, 7613 (1997).
- ³⁰K. R. Asmis, T. R. Taylor, C. S. Xu, and D. M. Neumark, *J. Chem. Phys.* **109**, 4389 (1998).
- ³¹T. R. Taylor, K. R. Asmis, M. T. Zanni, and D. M. Neumark, *J. Chem. Phys.* **110**, 7607 (1999).
- ³²A. D. Becke, *J. Chem. Phys.* **98**, 1372 (1993).
- ³³C. Lee, W. Yang, and R. G. Parr, *Phys. Rev. B* **37**, 785 (1988).
- ³⁴M. J. Frisch *et al.*, GAUSSIAN 98, Gaussian, Inc., Pittsburgh, PA (1998).
- ³⁵G. Herzberg, *Infrared and Raman Spectra of Polyatomic Molecules* (Van Nostrand, New York, 1945).
- ³⁶G. Herzberg, *Spectra of Diatomic Molecules* (Van Nostrand, New York, 1950).
- ³⁷F. G. Amar and L. Perera, *Z. Phys. D: At., Mol. Clusters* **20**, 173 (1991).
- ³⁸X. N. Zheng, S. L. Fei, M. C. Heaven, and J. Tellinghuisen, *J. Chem. Phys.* **96**, 4877 (1992).
- ³⁹D. R. T. Appadoo, R. J. Leroy, P. F. Bernath, S. Gerstenkorn, P. Luc, J. Verges, J. Sinzelle, J. Chevillard, and Y. Daignaux, *J. Chem. Phys.* **104**, 903 (1996).
- ⁴⁰Z. Liu, H. Gomez, and D. M. Neumark, *Faraday Discuss.* **118**, 221 (2001).
- ⁴¹V. S. Batista and D. F. Coker, *J. Chem. Phys.* **110**, 6583 (1999).
- ⁴²M. A. Walsh, T. H. England, T. R. Dyke, and B. J. Howard, *Chem. Phys. Lett.* **142**, 265 (1987).
- ⁴³K. W. Jucks, Z. S. Huang, D. Dayton, R. E. Miller, and W. J. Lafferty, *J. Chem. Phys.* **86**, 4341 (1987).
- ⁴⁴K. W. Jucks, Z. S. Huang, R. E. Miller, G. T. Fraser, A. S. Pine, and W. J. Lafferty, *J. Chem. Phys.* **88**, 2185 (1988).
- ⁴⁵R. Wester, A. V. Davis, A. E. Bragg, and D. M. Neumark, *Phys. Rev. A* (submitted).